UNIZIK JOURNAL OF AGRICULTURAL AND BIOSYSTEMS ENGINEERING

Journal homepage: https://journals.unizik.edu.ng/ujabe/

UJABE

August (2026), 1(4): 8-30

**ISSN:3141-2912**

# MODELING AND OPTIMIZING THE CATALYTIC TRANSESTERIFICATION PARAMETERS IN BIODIESEL PRODUCTION FROM WATERMELON SEED OIL, USING RESPONSE SURFACE METHODOLOGY (RSM) APPROACH

**Umunna Muofunanya Francis[1*]; Nyorere Oderhowho[1]; Igbozulike Augustine Onyekachi[2]; Adepoju Patience Oyenike[1]; Eke Akachukwu Benjamin[2]; Ndirika Victor Ifeanyi Obiora[3] and Ndukwu Macmanus Chinenye[2]**

[1]*Department of Agricultural and Bio-System Engineering, Southern Delta University, Ozoro.*

[2]*Department of Agricultural and Bioresources Engineering, Michael Okpara University of Agriculture, Umudike.*

[3]*Department of Agricultural and Biosystems Engineering, Nnamdi Azikiwe University, Awka.*

**Corresponding Author's E-mail:* umunnamuofunanya25@gmail.com or umunnam@sdu.edu.ng

**Received:** 6th July 2026; **Accepted:** 6th August 2026; **Available Online:** 31st August 2026

**ABSTRACT**

The increasing global demand for sustainable energy sources has intensified research into alternative feedstocks and catalysts for biodiesel production. This study investigated the optimization of biodiesel production from watermelon (*Citrullus lanatus*) seed oil using a novel biogenic catalyst derived from coconut husk ash (CHA) through response surface methodology (RSM). The watermelon seed oil was extracted and characterized, while the coconut husk ash catalyst was synthesized, characterized, and applied in the transesterification process. A central composite design (CCD) under RSM was employed to evaluate the interactive effects of five key process variables: catalyst concentration (0.5-2.0 wt%), methanol-to-oil molar ratio (6:1-14:1), reaction time (1-5 hours), temperature (30-70°C), and agitation speed (100-500 rpm) on biodiesel yield. The quadratic model demonstrated high statistical significance with an $R^2$ value of 0.9933, adjusted $R^2$ of 0.9812, and adequate precision of 41.0811. The optimal conditions were determined as: catalyst concentration of 1.36 wt%, methanol-to-oil ratio of 9.49:1, reaction time of 3.01 hours, temperature of 50.97°C, and agitation speed of 239.44 rpm, achieving a predicted biodiesel yield of 77.79% with a desirability of 1.0. Analysis of variance (ANOVA) revealed that methanol-to-oil ratio, reaction time, temperature, and agitation speed significantly influenced biodiesel yield ($p < 0.05$). The produced biodiesel exhibited favorable fuel properties including kinematic viscosity of 9.372 $mm^2/s$ at 40°C, flash point of 164°C, cetane number of 50.97, and calorific value of 44.565 MJ/kg. Characterization via FTIR and GC-MS confirmed the successful conversion of triglycerides to fatty acid methyl esters (FAMEs) with dominant peaks corresponding to methyl palmitate, methyl oleate, and methyl linoleate. This study demonstrates the viability of watermelon seed oil as a non-edible feedstock and coconut husk ash as a cost-effective, environmentally friendly heterogeneous catalyst for sustainable biodiesel production.

**Keywords:** Biodiesel; Response Surface Methodology; Watermelon Seed Oil; Coconut Husk Ash; Transesterification; Optimization

## 1.0 INTRODUCTION

The depletion of fossil fuel reserves and growing environmental concerns regarding greenhouse gas emissions has accelerated the search for renewable and sustainable energy alternatives (Akram *et al*., 2021). Biodiesel, a biodegradable, non-toxic, and renewable fuel derived from vegetable oils and animal fats, has emerged as a promising substitute for petroleum-based diesel (Elumalai *et al*., 2021; Muhammad *et al*., 2015). Global biodiesel production reached approximately 36 billion liters in 2017, with projections indicating a 9% increase by 2027 (OECD/FAO, 2018). However, the widespread commercialization of biodiesel faces significant challenges, primarily

related to elevated production costs and feedstock availability (Liu *et al*., 2012; Tamoradi *et al*., 2021). Conventional biodiesel production relies heavily on edible vegetable oils, which account for over 80% of production costs (Jan *et al*., 2023). This economic constraint has redirected research attention toward non-edible feedstocks such as waste cooking oils, Jatropha oil, algae, and various seed oils (Esonye *et al*., 2019; Olatunji *et al*., 2021). Watermelon (*Citrullus lanatus*) seed oil has recently gained attention as a promising non-edible feedstock due to its favorable fatty acid composition, abundant availability as agricultural waste, and potential for sustainable biodiesel production (Iweka *et al*., 2023; Nwufo *et al.*, 2023). The transesterification process, which converts triglycerides to fatty acid methyl esters (FAMEs) in the presence of an alcohol and catalyst, remains the most widely adopted method for biodiesel production (Çakırca & Akın, 2021; Khan *et al*., 2021). While homogeneous base catalysts (NaOH, KOH) offer high reaction rates and conversion efficiencies, they present several disadvantages including corrosiveness, difficulty in separation and recovery, soap formation with high free fatty acid (FFA) feedstocks, and generation of substantial wastewater (Aderibigbe *et al*., 2021; Mansir *et al*., 2021). These limitations have prompted extensive research into heterogeneous catalysts derived from waste materials, offering advantages such as reusability, ease of separation, reduced corrosiveness, and environmental sustainability (Nadeem *et al*., 2021; Saman *et al*., 2021). Agricultural waste-derived catalysts, including mollusk shells, eggshells, calcined fish scales, and coconut husk ash, have demonstrated promising catalytic activity in biodiesel production (Idris *et al*., 2021; Mohadesi *et al*., 2021). Coconut husk, a widely available agricultural residue, possesses a lignocellulosic structure that, upon thermal treatment, yields a porous, high-surface-area material with basic active sites suitable for transesterification reactions (Husin *et al*., 2018; Pradana *et al*., 2018). The utilization of such waste-derived catalysts aligns with circular economy principles and reduces overall production costs. Response surface methodology (RSM) has emerged as an effective statistical technique for optimizing biodiesel production processes, enabling the evaluation of interactive effects among multiple variables with minimal experimental runs (Betiku *et al*., 2015; Dhingra *et al*., 2013). Central composite design (CCD), a widely used RSM approach, facilitates the development of predictive quadratic models and identification of optimal process conditions (Moatamed *et al.*, 2021; Akinfalabi *et al*., 2020). This study aims to investigate the application of RSM for modeling and optimizing transesterification parameters in biodiesel production from watermelon seed oil catalyzed by biogenic coconut husk ash. The specific objectives include: (1) extraction and characterization of watermelon seed oil; (2) synthesis and characterization of coconut husk ash catalyst; (3) evaluation of process parameter effects on biodiesel yield; (4) optimization of reaction conditions using CCD-RSM; and (5) characterization of the produced biodiesel. The findings of this research will contribute to the development of sustainable biodiesel production pathways utilizing non-edible feedstocks and waste-derived catalysts.

## 2.0 METHODOLOGY

### 2.1 Materials

Watermelon seeds were collected from fruit vendor waste bins at Ndioru market in Ikwuano Local Government Area, Abia State, Nigeria. Coconut husks were obtained from Ndioru village, Abia State. Methanol (analytical grade, 99.8% purity) was procured from Merck (Mumbai, India). All other solvents and chemicals used were of analytical grade and employed without further purification. The experiments were conducted at Biochem Analytics LTD, Enugu, Nigeria.

### 2.2 Sample Preparation and Oil Extraction

The watermelon seeds were thoroughly washed to remove soluble particles, dust, and contaminants, followed by sun-drying for 72 hours. The dried seeds were crushed to uniform particle size using a laboratory blender and stored in sealed containers prior to oil extraction. Oil extraction was performed using the Soxhlet extraction method following the procedure described by Ude *et al*. (2020). One hundred grams (100 g) of the ground sample was weighed into a cellulose thimble and placed in a Soxhlet extractor. Two hundred and fifty milliliters (250 mL) of n-hexane was measured into a 500 mL flat-bottom round flask. The extraction setup was assembled with a condenser and heated using a heating mantle at 65°C for 6 hours. The solvent was separated from the oil using a rotary vacuum evaporator (Laborota 4000) at 40°C. The extracted oil was weighed, and the oil yield was calculated using Equation (1):

$$Y = \frac{W_o}{W} \times 100 \quad \ldots\ldots\ldots\ldots\ldots\ldots\ldots\ldots \quad (1)$$

Where, Y is the oil yield (%),
$W_o$ is the weight of oil extracted (g) and
W is the weight of initial sample (g)

### 2.3 Characterization of Watermelon Seed Oil

The physicochemical properties of the extracted oil were determined using standard methods according to ASTM E3146 (2024) and ASTM D6751 (2025) guidelines. The following properties were evaluated:

i. **Kinematic Viscosity**: Determined at 40°C using a digital viscometer (Searchtech Instruments, England) following ASTM D445.
ii. **Specific Gravity**: Measured using a 25 mL specific gravity bottle at 25°C according to ASTM D4052.
iii. **Acid Value**: Determined by titration with 0.1 N KOH according to ASTM D664.
iv. **Free Fatty Acid (FFA) Value**: Calculated from acid value using the relationship FFA = AV × 0.503.
v. **Saponification Value**: Determined by refluxing the oil with 0.5 N ethanolic KOH followed by back-titration with HCl according to ASTM D5558.
vi. **Peroxide Value**: Determined by titration with sodium thiosulfate according to ASTM D154.

vii. **Moisture Content**: Determined by oven drying at 105°C according to ASTM D95.
viii. **Ester Value**: Calculated as the difference between saponification value and acid value.

The molecular weight of the oil was calculated based on the fatty acid profile obtained from GC-MS analysis using Equation (2):

$$\text{MW. of a triglyceride} = 3 \times \text{Average MW.} + 38.049 \quad (2)$$

Where,

$3 =$ Number of chains of each fatty acid in a triglyceride

$38.049 =$ Molecular mass of glycerol in the triglyceride (Glycerol backbone)

### 2.4 Instrumental Characterization of Oil

**Fourier Transform Infrared (FTIR) Spectroscopy**: Functional groups present in the watermelon seed oil were identified using a Shimadzu FTIR-8400S spectrophotometer in the mid-infrared region (500-5000 $cm^{-1}$) with potassium bromide (KBr) discs. A spectral resolution of 2 $cm^{-1}$ was employed.

**Gas Chromatography-Mass Spectrometry (GC-MS)**: Fatty acid composition was determined using a Thermofinnigan Trace GC/Trace DSQ/A1300 equipped with an SGE-BPX5 MS fused silica capillary column (film thickness 0.25 μm). Helium was used as carrier gas at a flow rate of 10 mL/min. The injector and MS transfer line temperatures were set at 220°C and 290°C, respectively. The oven temperature was programmed from 50°C to 150°C at 3°C/min, held isothermally for 100 minutes, then raised to 250°C at 10°C/min.

**Thermogravimetric Analysis (TGA)**: Thermal stability was evaluated using a Mettler-Toledo TG850 thermo-analyzer under high-purity nitrogen gas at a flow rate of 5.0 L/h, with a heating rate of 10°C/min over a temperature range of 0-1000°C.

### 2.5 Synthesis and Characterization of Coconut Husk Ash Catalyst

**Preparation**: Coconut husk ash was prepared following the method of Rafiee et al. (2012). The husks were thoroughly washed, dried at 110°C for 24 hours, and calcined at 1000°C for 4 hours in a muffle furnace. The resulting ash was ground to fine powder and sieved through a 150 μm mesh.

**Catalyst Characterization**:

i. **FTIR**: Functional groups were identified using the same FTIR protocol as for the oil sample.
ii. **Scanning Electron Microscopy (SEM)**: Surface morphology was examined using a JEOL-JSM 760F scanning electron microscope.

iii. **X-Ray Diffraction (XRD)**: Crystalline phases were identified using a Shimadzu XRD-7000 diffractometer with Cu Kα radiation (40 kV, 30 mA, λ = 1.5418 Å) over a 2θ range of 3-40° at a scanning speed of 2°/min.

iv. **Brunauer-Emmett-Teller (BET)**: Surface area, pore volume, and pore diameter were determined using a Micromeritics ASAP 2020 surface analyzer via nitrogen adsorption at 77 K.

### 2.6 Transesterification Reaction

The transesterification reaction was conducted in a 250 mL three-neck round-bottom flask equipped with a condenser, thermometer, and magnetic stirrer. A predetermined amount of catalyst (0.5-2.5 wt% of oil) was mixed with methanol (6:1-14:1 molar ratio) and added to the oil sample (50 g). The reaction mixture was heated to the desired temperature (30-70°C) with continuous stirring (100-500 rpm) for a specified time (1-5 hours). Upon completion, the mixture was transferred to a separating funnel and allowed to settle overnight at room temperature. The biodiesel layer (upper phase) was separated from glycerol (lower phase) and washed with warm distilled water to remove residual catalyst and methanol. The biodiesel was dried over anhydrous sodium sulfate, and the yield was calculated using Equation (3):

$$Yield = \frac{Wb}{Wo} x\ 100 \quad \ldots\ldots\ldots\ldots\ldots\ldots\ (3)$$

Where: Wb = Weight of biodiesel
Wo = Weight of oil used

### 2.7 Experimental Design and Optimization

A central composite design (CCD) under response surface methodology was employed to optimize the transesterification parameters using Design Expert software version 13.0.6 (Stat-Ease Inc., Minneapolis, USA). Five independent variables at three levels were investigated:

**Table 1: Experimental Optimization Data**

| Variable | Symbol | Units | Coded Levels | | | | |
|---|---|---|---|---|---|---|---|
| | | | -2 | -1 | 0 | +1 | +2 |
| **Catalyst Concentration** | A | wt% | 0.5 | 1.0 | 1.5 | 2.0 | 2.5 |
| **Methanol/Oil Ratio** | B | mol/mol | 6:1 | 8:1 | 10:1 | 12:1 | 14:1 |
| **Reaction Time** | C | Hours | 1 | 2 | 3 | 4 | 5 |
| **Temperature** | D | °C | 30 | 40 | 50 | 60 | 70 |
| **Agitation Speed** | E | Rpm | 100 | 200 | 300 | 400 | 500 |

The experimental design consisted of 32 runs, including five replicates at the center point. The response variable was biodiesel yield (%). The quadratic model was expressed as:

$$Y = \beta_0 + \sum_{i=1}^{5} \beta_i X_i + \sum_{i=1}^{5} \beta_{ii} X^2{}_i + \sum_{i=1}^{5} \sum_{j=i+1}^{5} \beta_{ij} X_i X_j \quad \ldots\ldots\ldots\ldots\ldots\ldots\ (4)$$

Where Y is the predicted response, $\beta_0$ is the intercept, $\beta_i$ are linear coefficients, $\beta_{ii}$ are quadratic coefficients, $\beta_{ij}$ are interaction coefficients, and $X_i$ are coded independent variables.

### 2.8 Characterization of Optimal Biodiesel

The biodiesel produced under optimal conditions was characterized for fuel properties according to ASTM D6751 and EN 14214 standards:

i. **Kinematic Viscosity**: ASTM D445 at 40°C
ii. **Density**: ASTM D4052 at 15°C
iii. **Flash Point**: ASTM D93 (Pensky-Martens closed cup)
iv. **Cloud Point**: ASTM D2500
v. **Cetane Number**: ASTM D613
vi. **Calorific Value**: ASTM D240
vii. **FTIR Analysis**: Identification of functional groups
viii. **GC-MS Analysis**: Fatty acid methyl ester composition

## 3.0 Results and Discussion

### 3.1 Characterization of Watermelon Seed Oil

The physicochemical properties of the extracted watermelon seed oil are presented in Table 2. The oil yield was 45.6%, indicating good extractability and potential as a biodiesel feedstock.

**Table 2: Physicochemical Properties of Watermelon Seed Oil**

| Property | Measured Value |
|---|---|
| **Kinematic Viscosity @ 40°C (mm²/s)** | 28.448 |
| **Refractive Index @ 33°C** | 1.4702 |
| **Acid Value (mg KOH/g)** | 12.933 |
| **Free Fatty Acid Value (mg KOH/g)** | 6.4665 |
| **Moisture Content (%)** | 0.7540 |
| **Saponification Value (mg KOH/g)** | 347.820 |
| **Peroxide Value (meq/kg)** | 2.187 |
| **Specific Gravity** | 0.9232 |
| **Molecular Weight (g/mol)** | 502.558 |
| **Ester Value (%)** | 96.282 |

The kinematic viscosity of 28.448 mm²/s at 40°C falls within the range typical for vegetable oils, though somewhat lower than the 35.355 mm²/s reported by Adam *et al*. (2025). The lower viscosity observed in this study may indicate a higher degree of unsaturation in the triglyceride composition, reducing intermolecular forces and facilitating easier flow. Since viscosity influences combustion efficiency and atomization in biodiesel applications, the result suggests that watermelon seed oil could be a viable feedstock, although blending or modification may be required to meet ASTM and EN biodiesel standards. The acid value of 12.933 mg KOH/g is significantly higher than the 6.47 mg KOH/g reported by Adam *et al*. (2025). Oils with acid values exceeding 4 mg KOH/g are generally considered unsuitable for edible purposes without refining, as recommended by FAO/WHO standards. The elevated acid value suggests possible degradation due to prolonged storage or high initial moisture content, making pretreatment necessary before biodiesel production. The FFA value of 6.4665 mg KOH/kg further supports evidence of hydrolytic breakdown, indicating that an esterification pretreatment would be required to lower the FFA before transesterification. The moisture content of 0.754% is

moderately high compared to values below 0.5% reported in literature for well-preserved seed oils (Ibrahim *et al*., 2023). Excess moisture accelerates hydrolysis, thereby increasing FFA and acid values over time. The higher moisture content likely contributed to the elevated acid and FFA values recorded. Low moisture content is a critical requirement for biodiesel feedstock to avoid catalyst deactivation and unwanted side reactions. The saponification value of 347.820 mg KOH/kg indicates the presence of relatively lower molecular weight triglycerides and/or a significant proportion of short to medium chain fatty acids. This high value suggests higher reactivity with base, which is favorable for transesterification reactions (Moaddabdoost Baboli and Kordi, 2010). The peroxide value of 2.187 meq/kg indicates a relatively low level of primary oxidation products, suggesting acceptable oxidative stability for practical applications (Popoola and Haruna, 2024). The specific gravity of 0.9232 is typical for many vegetable oils, reflecting moderate unsaturation and absence of large amounts of non-lipid constituents.

## 3.2 RSM Modeling and Optimization

### 3.2.1 Model Development and Statistical Analysis

The CCD experimental matrix and corresponding biodiesel yields are presented in Table 3. The yields ranged from 53.1% to 88.4%, indicating that process parameters significantly influenced the transesterification reaction. The maximum yield of 88.4% occurred at a catalyst concentration of 1.5 wt%, methanol-to-oil ratio of 6:1, reaction time of 3 hours, temperature of 50°C, and agitation speed of 300 rpm.

**Table 3: CCD Experimental Matrix and Biodiesel Yields**

| Run | Catalyst Conc. (wt%) | Methanol/Oil Ratio | Time (h) | Temp (°C) | Agitation (rpm) | Yield (%) |
|---|---|---|---|---|---|---|
| **1** | 1.0 | 8 | 2 | 40 | 400 | 70.6 |
| **2** | 2.0 | 8 | 2 | 40 | 200 | 68.0 |
| **3** | 1.0 | 12 | 2 | 40 | 200 | 73.4 |
| **4** | 2.0 | 12 | 2 | 40 | 400 | 69.3 |
| **5** | 1.0 | 8 | 2 | 60 | 200 | 77.9 |
| **6** | 2.0 | 8 | 2 | 60 | 400 | 58.8 |
| **7** | 1.0 | 12 | 2 | 60 | 400 | 75.7 |
| **8** | 2.0 | 12 | 2 | 60 | 200 | 71.5 |
| **9** | 1.0 | 8 | 4 | 40 | 200 | 83.6 |
| **10** | 2.0 | 8 | 4 | 40 | 400 | 73.6 |
| **11** | 1.0 | 12 | 4 | 40 | 400 | 56.2 |
| **12** | 2.0 | 12 | 4 | 40 | 200 | 60.0 |
| **13** | 1.0 | 8 | 4 | 60 | 400 | 65.7 |
| **14** | 2.0 | 8 | 4 | 60 | 200 | 76.9 |
| **15** | 1.0 | 12 | 4 | 60 | 200 | 70.1 |
| **16** | 2.0 | 12 | 4 | 60 | 400 | 68.4 |
| **17** | 0.5 | 10 | 3 | 50 | 300 | 75.9 |
| **18** | 2.5 | 10 | 3 | 50 | 300 | 73.1 |
| **19** | 1.5 | 6 | 3 | 50 | 300 | 88.4 |
| **20** | 1.5 | 14 | 3 | 50 | 300 | 79.1 |
| **21** | 1.5 | 10 | 3 | 30 | 300 | 65.3 |
| **22** | 1.5 | 10 | 3 | 70 | 300 | 66.3 |

| | | | | | | |
|---|---|---|---|---|---|---|
| **23** | 1.5 | 10 | 1 | 50 | 300 | 75.9 |
| **24** | 1.5 | 10 | 5 | 50 | 300 | 76.2 |
| **25** | 1.5 | 10 | 3 | 50 | 100 | 61.0 |
| **26** | 1.5 | 10 | 3 | 50 | 500 | 53.1 |
| **27-32** | 1.5 | 10 | 3 | 50 | 300 | 76.4 |

The quadratic model developed for biodiesel yield in terms of coded factors is presented in Equation (5):

**Biodiesel Yield (%) =** +76.22 +0.3109A -8.72B -3.97C +1.40D -7.46E +2.68AB +7.80AC -0.1688AD +5.72AE -18.66BC +10.83BD +8.07BE +1.59CD -3.22CE -3.12DE -1.15$A^2$ +7.20$B^2$ -0.7813$C^2$ -10.75$D^2$ -19.50$E^2$ (5)

Where A, B, C, D, and E represent coded values for catalyst concentration, methanol/oil ratio, reaction time, temperature, and agitation speed, respectively.

### 3.2.2 ANOVA Analysis

The ANOVA results for the quadratic model are presented in Table 4. The high F-value (81.89) and low p-value (<0.0001) indicate that the model is statistically significant. The lack of fit was not significant ($p > 0.05$), confirming that the model adequately fits the experimental data.

**Table 4: ANOVA Results for Biodiesel Yield Model**

| Source | Sum of Squares | Df | Mean Square | F-value | p-value |
|---|---|---|---|---|---|
| **Model** | 1884.76 | 20 | 94.24 | 81.89 | <0.0001 |
| **A-Catalyst conc.** | 0.4702 | 1 | 0.4702 | 0.4086 | 0.5358 |
| **B-Methanol/oil ratio** | 260.50 | 1 | 260.50 | 226.38 | <0.0001 |
| **C-Time** | 27.54 | 1 | 27.54 | 23.93 | 0.0005 |
| **D-Temperature** | 6.72 | 1 | 6.72 | 5.84 | 0.0342 |
| **E-Agitation Speed** | 190.72 | 1 | 190.72 | 165.73 | <0.0001 |
| **AB** | 12.78 | 1 | 12.78 | 11.11 | 0.0067 |
| **AC** | 69.31 | 1 | 69.31 | 60.23 | <0.0001 |
| **AD** | 0.0506 | 1 | 0.0506 | 0.0440 | 0.8377 |
| **AE** | 58.14 | 1 | 58.14 | 50.52 | <0.0001 |
| **BC** | 222.76 | 1 | 222.76 | 193.57 | <0.0001 |
| **BD** | 117.18 | 1 | 117.18 | 101.83 | <0.0001 |
| **BE** | 65.21 | 1 | 65.21 | 56.66 | <0.0001 |
| **CD** | 1.63 | 1 | 1.63 | 1.41 | 0.2596 |
| **CE** | 6.63 | 1 | 6.63 | 5.76 | 0.0352 |
| **DE** | 9.77 | 1 | 9.77 | 8.49 | 0.0141 |
| **$A^2$** | 7.70 | 1 | 7.70 | 6.70 | 0.0252 |
| **$B^2$** | 95.04 | 1 | 95.04 | 82.59 | <0.0001 |
| **$C^2$** | 0.4583 | 1 | 0.4583 | 0.3983 | 0.5409 |
| **$D^2$** | 211.86 | 1 | 211.86 | 184.11 | <0.0001 |
| **$E^2$** | 697.13 | 1 | 697.13 | 605.80 | <0.0001 |
| **Residual** | 12.66 | 11 | 1.15 | | |

| | | | | | |
|---|---|---|---|---|---|
| **Lack of Fit** | 12.66 | 6 | 2.11 | | |
| **Pure Error** | 0.0000 | 5 | 0.0000 | | |
| **Cor Total** | 1897.42 | 31 | | | |
| **Std. Dev.** | 1.07 | $R^2$ = 0.9933 | Adjusted $R^2$ = 0.9812 | Predicted $R^2$ = 0.8214 | Adeq Precision = 41.0811 |

The coefficient of determination ($R^2$ = 0.9933) indicates that the model explains 99.33% of the variability in biodiesel yield. The adjusted $R^2$ (0.9812) is in reasonable agreement with the predicted $R^2$ (0.8214), confirming the model's adequacy. The adequate precision value of 41.0811 (greater than 4) indicates an adequate signal-to-noise ratio, demonstrating the model's desirability for navigating the design space. The linear terms (B, C, D, and E), quadratic terms ($A^2$, $B^2$, $D^2$, and $E^2$), and interactive effects (AB, AC, AE, BC, BD, BE, CE, and DE) were all significant ($p < 0.05$) in the biodiesel yield response model. The positive and negative signs in Equation (5) indicate the direction of effect on the response. Increased A, D, AB, AC, AE, BD, BE, CD, and $B^2$ led to increased response, while increased B, C, E, AD, BC, CE, DE, $A^2$, $C^2$, $D^2$, and $E^2$ resulted in decreased response.

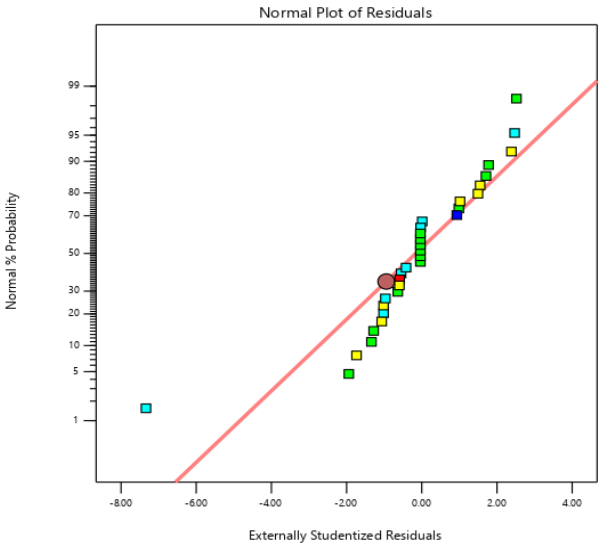


**Figure 1: Normal % probability vs. internal studentized residuals.**

The normal probability plot of residuals (Figure 1) showed points distributed along a straight diagonal line, indicating that the residuals followed a normal distribution.

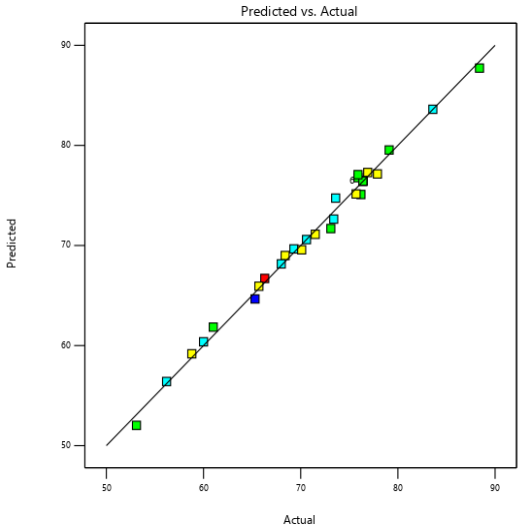


**Figure 2: Predicted vs. Actual values of the model on biodiesel yield**

The predicted versus actual values plot (Figure 2) revealed a straight line, confirming good agreement between experimental and predicted values.

### 3.3 Interaction Effects of Process Parameters

#### 3.3.1 Effect of Catalyst Concentration and Methanol/Oil Ratio (AB)

Figure 3 illustrates the interaction between catalyst concentration and methanol/oil ratio on biodiesel yield. At low methanol/oil ratios (6:1), yield was relatively high, but as the ratio increased to 12:1, yield initially dropped before rising again at higher ratios. This suggests that excessive methanol can cause reversal of the reaction or dilute reactants, while very high methanol content can drive the reaction to completion. Similarly, increasing catalyst concentration from 0.5 wt% to 1.5 wt% improved yield significantly, but beyond approximately 1.7 wt%, further increases did not lead to proportional improvements and could even have negative effects due to soap formation (Anas *et al*., 2024; Atabani *et al*., 2012).

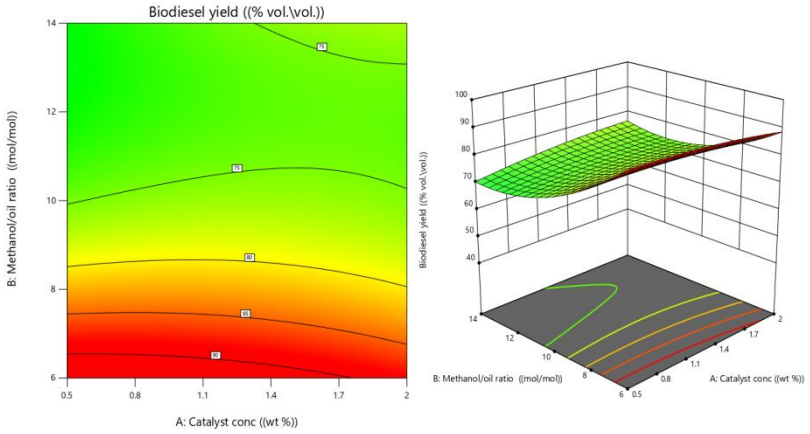


**Figure 3: Contour and 3D plots on the effect of catalyst concentration and methanol/oil**

### 3.3.2 Effect of Catalyst Concentration and Time (AC)

Figure 4 shows the interaction between catalyst concentration and reaction time. Lower catalyst concentrations (<1 wt%) resulted in relatively low biodiesel yields (50-65%), especially at shorter reaction times. Increasing catalyst concentration to 1.5-1.7 wt% improved yield significantly, approaching 75-85%, but further increases showed diminishing returns. The optimal catalyst range was around 1.5-1.7 wt%, above which side reactions such as soap formation could occur. Biodiesel yield improved with longer reaction times, especially from 1 to 4 hours, beyond which the change in yield was minimal (Nizami *et al*., 2020).

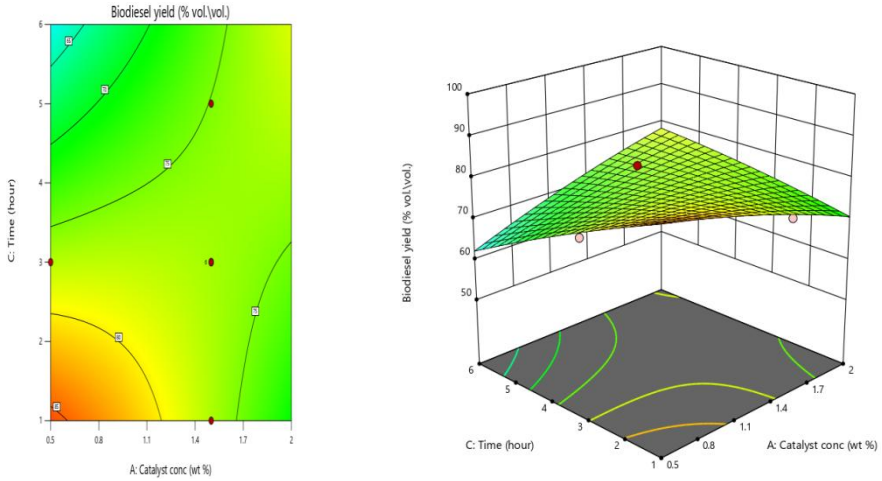


**Figure 4: Contour and 3D plots on the effect of catalyst concentration and time on biodiesel yield**

### 3.3.3 Effect of Catalyst Concentration and Temperature (AD)

Figure 5 shows the interaction between catalyst concentration and temperature. Increasing catalyst concentration from 0.5% to 1.5% increased biodiesel yield, reaching a peak and then slightly decreasing at higher concentrations. Similarly, yield increased with temperature up to an optimum around 55-60°C, after which it declined due to methanol evaporation and potential biodiesel degradation (Baskar *et al*., 2019).

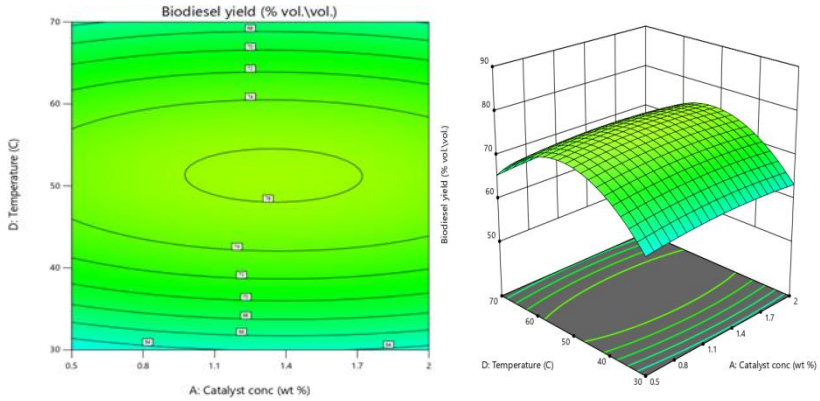


**Figure 5: Contour and 3D plots on the effect of catalyst concentration and temperature on biodiesel yield**

### 3.3.4 Effect of Catalyst Concentration and Agitation Speed (AE)

Figure 6 shows the interaction between catalyst concentration and agitation speed. Yield

increased significantly with increasing catalyst concentration from 0.5% to 1.5%, beyond which further increases resulted in diminishing returns. Agitation speed up to 300-350 rpm improved yield, beyond which the yield dropped slightly due to shear degradation, air entrainment, or ineffective mixing at higher speeds (Baskar *et al*., 2019).

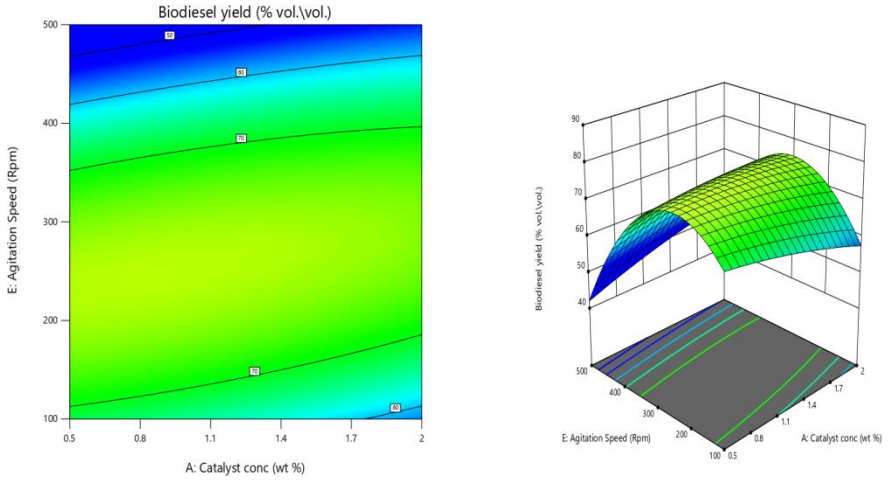


**Figure 6: Contour and 3D plots on the effect of catalyst concentration and agitation speed on biodiesel yield**

### 3.3.5 Effect of Methanol/Oil Ratio and Time (BC)

Figure 7 shows the interaction between methanol/oil ratio and time. At low methanol/oil ratios (6:1), yield was relatively high. As the ratio increased beyond 9:1, the yield initially dropped before rising again beyond 12:1. Short reaction times (<2 hours) resulted in low yields, while longer times (5-6 hours) generally favored higher yields, as more triglycerides were converted to methyl esters (Baskar and Aiswarya, 2016).

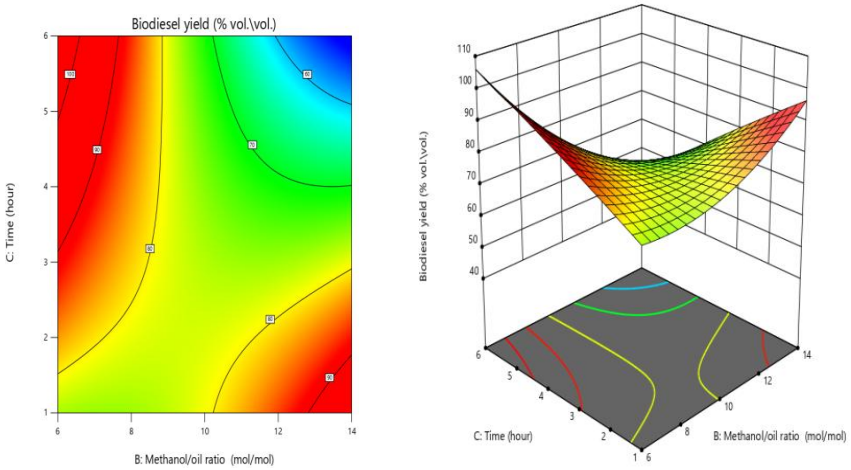


**Figure 7: Contour and 3D plots on the effect of methanol/oil ratio and time on biodiesel yield**

### 3.3.6 Effect of Methanol/Oil Ratio and Temperature (BD)

Figure 8 shows the interaction between methanol/oil ratio and temperature. At lower methanol/oil ratios (6-8) and moderate temperatures (50-60°C), biodiesel yield increased significantly. Beyond optimal values, especially at high methanol ratios (14) or lower temperatures (<40°C), yield declined due to excess methanol diluting reactants or insufficient temperature reducing reaction kinetics (Baskar *et al*., 2019; Rajia *et al*., 2023).

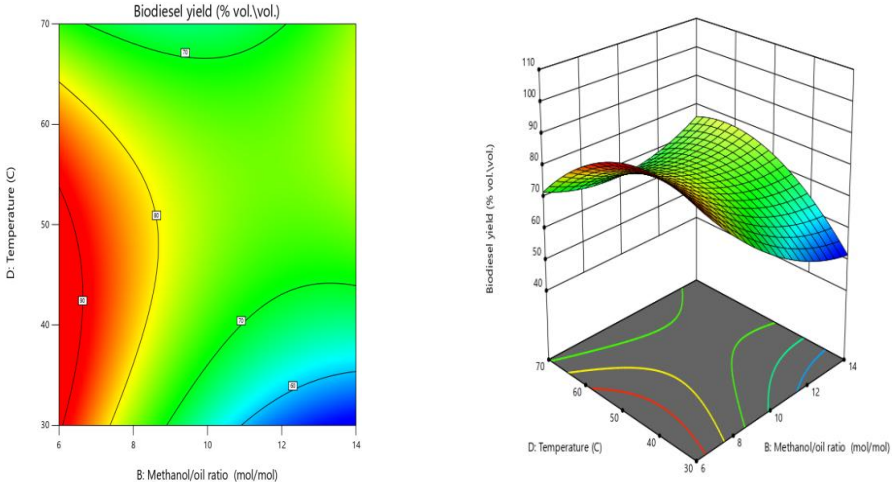


**Figure 8: Contour and 3D plots on the effect of methanol/oil ratio and temperature on biodiesel yiel**

### 3.3.7 Effect of Methanol/Oil Ratio and Agitation Speed (BE)

Figure 9 shows the interaction between methanol/oil ratio and agitation speed. At lower methanol/oil ratios (6-8), yield increased with increasing agitation speed up to 300-400 rpm. At high methanol/oil ratios (>12), yield declined even at higher agitation speeds. Peak biodiesel yields (80-90%) occurred at moderate methanol/oil ratio (9-10 mol/mol) and agitation speed (300 rpm). High methanol/oil ratio combined with low agitation led to low yields, emphasizing the need for optimizing both factors (Baskar and Aiswarya, 2016; Oladipo *et al*., 2022).

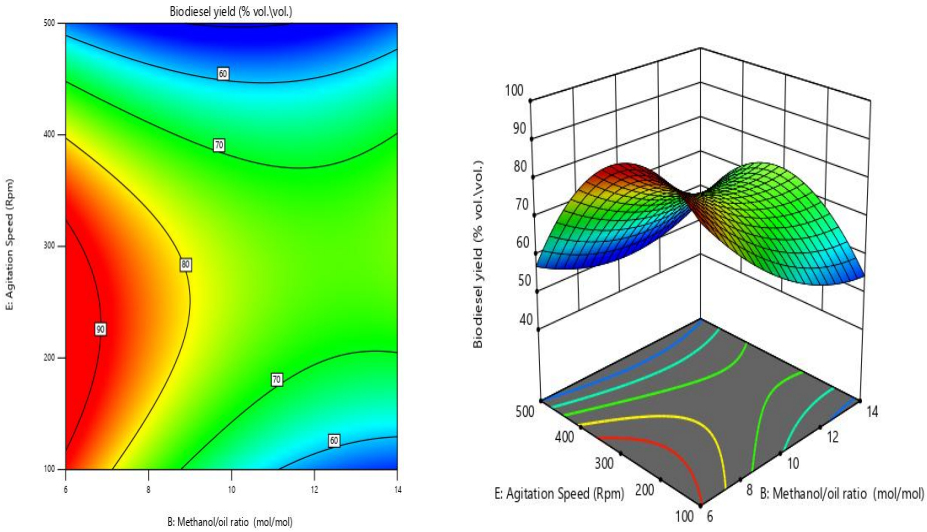


**Figure 9: Contour and 3D plots on the effect of methanol/oil ratio and agitation speed on biodiesel yield**

### 3.3.8 Effect of Time and Temperature (CD)

Figure 10 shows the interaction between reaction time and temperature. Yield increased with reaction time up to about 4 hours, beyond which the curve flattened. Temperature increase enhanced the yield up to an optimum of around 55°C, after which the effect diminished or reversed. These findings align with previous studies where optimal reaction times between 3-4 hours and temperatures around 50-60°C are recommended for efficient biodiesel production (Gaurav *et al*., 2021; Tanimu *et al*., 2018).

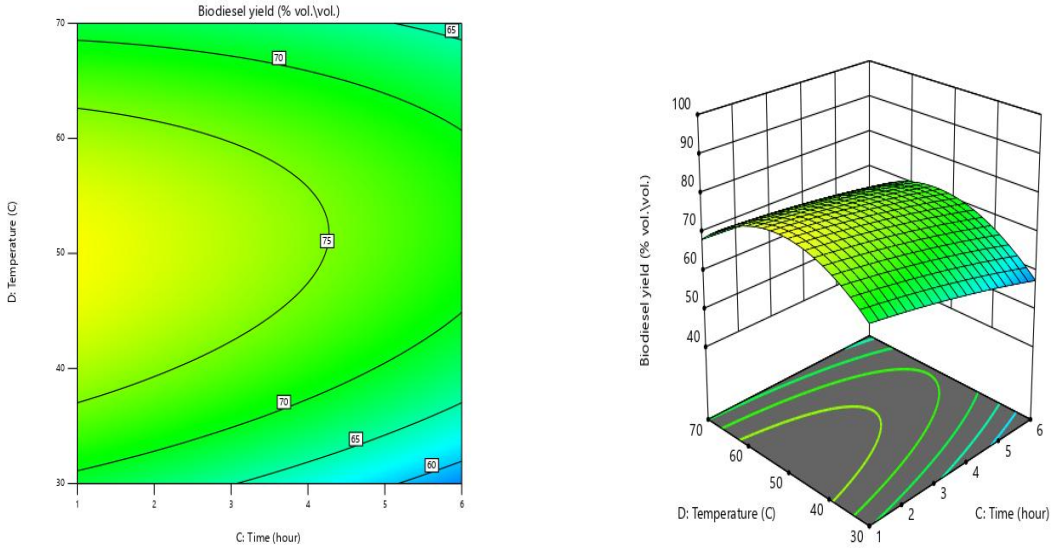


**Figure 10: Contour and 3D plots on the effect of time and temperature on biodiesel yield**

### 3.3.9 Effect of Time and Agitation Speed (CE)

Figure 11 shows the interaction between reaction time and agitation speed. Optimum biodiesel yield (70%) was achieved around 390 rpm agitation speed and 5 hours' reaction time. At low agitation speeds (100-200 rpm), yield remained lower (50-55%). As agitation speed increased to 400 rpm, yield improved significantly to 65-70%. Beyond 400 rpm, the surface began to decline slightly, suggesting that excessive agitation does not further enhance mass transfer and may even cause turbulence, entrainment of air, and soap formation. While at shorter times of 1-2 hours, yields were comparatively low, and as reaction time increased to 5 hours, yields improved (ASTM International, 2025; Narayan and Arjun, 2021).

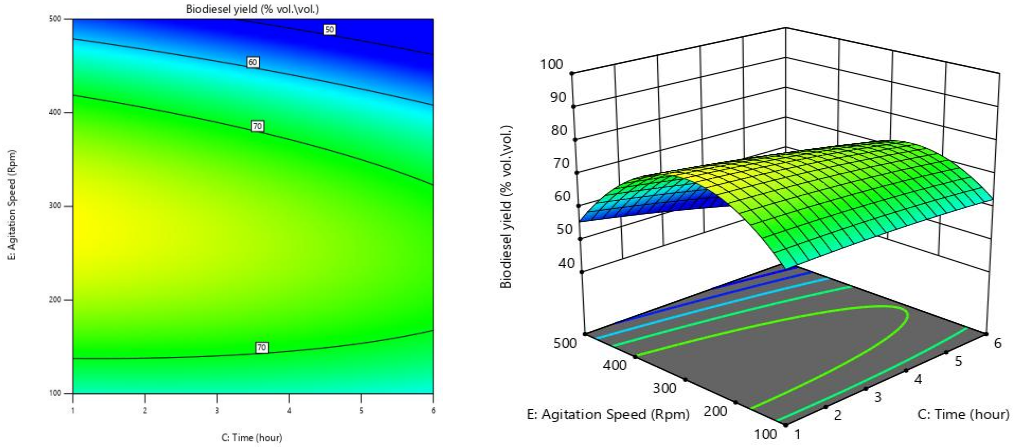


**Figure 11: Contour and 3D plots on the effect of time and agitation speed on biodiesel yield**

### 3.3.10 Effect of Temperature and Agitation Speed (DE)

Figure 12 shows the interaction between temperature and agitation speed. At low agitation speeds (100-200 rpm), yield was relatively low (40-50%) due to insufficient mixing. As agitation speed increased from 200 to 400 rpm, yield significantly improved (60-70%), indicating enhanced mass transfer. Beyond 400 rpm, further increases did not enhance yield. At lower temperatures (30-40°C), yield was poor (<50%) due to reduced reaction kinetics. With increasing temperature (50-60°C), yield improved (65-70%). Above 60°C, the yield slightly reduced due to methanol evaporation and possible side reactions (Adams *et al*., 2025).

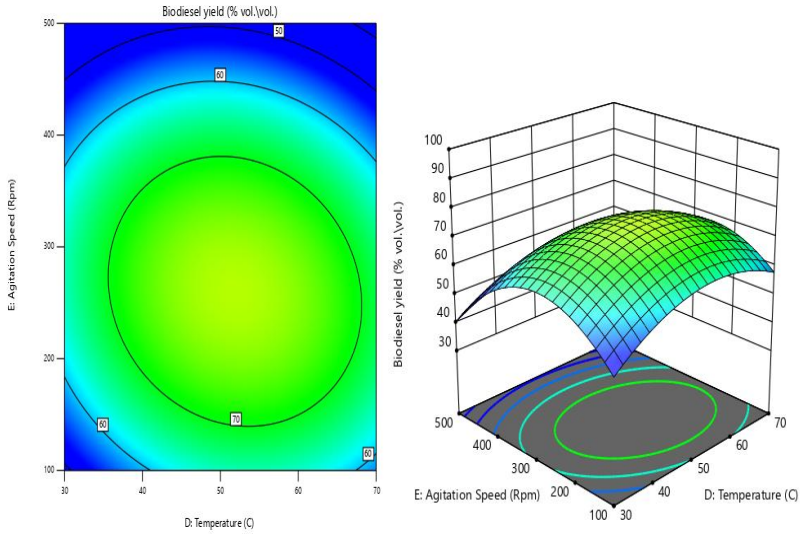


**Figure 12: Contour and 3D plots on the effect of temperature and agitation speed on biodiesel yield**

## 3.4 Process Optimization

The numerical optimization using the desirability function approach identified the optimal conditions for biodiesel production. The constraints applied for optimization are presented in Table 5.

**Table 5: Optimization Constraints**

| Name | Goal | Lower Limit | Upper Limit | Importance |
|---|---|---|---|---|
| **A:Catalyst conc.** | In range | 0.5 | 2.0 | 3 |
| **B:Methanol/oil ratio** | In range | 6 | 14 | 3 |
| **C:Time** | In range | 1 | 5 | 3 |
| **D:Temperature** | In range | 30 | 70 | 3 |
| **E:Agitation Speed** | In range | 100 | 500 | 3 |
| **Biodiesel yield** | In range | 53.1 | 88.4 | 3 |

The optimal conditions predicted by the model were: catalyst concentration of 1.36 wt%, methanol/oil ratio of 9.49:1, reaction time of 3.01 hours, temperature of 50.97°C, and agitation speed of 239.44 rpm. These conditions yielded a predicted biodiesel yield of 77.79% with a desirability of 1.0 (Figures 1 and 2). The predicted values were validated experimentally, showing good agreement with the model predictions, confirming the reliability of the optimized conditions.

### 3.5 Characterization of Optimal Biodiesel

#### 3.5.1 Physicochemical Properties

The fuel properties of the biodiesel produced under optimal conditions are presented in Table 6.

**Table 6: Fuel Properties of Optimal Biodiesel**

| Property | Measured Value |
|---|---|
| **Kinematic Viscosity @ 40°C ($mm^2/s$)** | 9.372 |
| **Density ($kg/m^3$)** | 0.8798 |
| **Flash Point (°C)** | 164.00 |
| **Smoke Point (°C)** | 100.00 |
| **Cloud Point (°C)** | 6.50 |
| **Moisture (%)** | 0.076 |
| **Aniline Point (°F)** | 184.00 |
| **Diesel Index** | 53.97 |
| **API Gravity** | 29.33 |
| **Cetane Number** | 50.97 |
| **Calorific Value (MJ/kg)** | 44.565 |

The kinematic viscosity of 9.372 $mm^2/s$ at 40°C is higher than typical biodiesel standards (ASTM D6751: 1.9-6.0 $mm^2/s$; EN 14214: 3.5-5.0 $mm^2/s$), which may indicate incomplete transesterification or presence of residual glycerides (Knothe, 2005). This elevated viscosity could impair fuel atomization and injection in diesel engines, suggesting that further purification or blending with low-viscosity components may be necessary (El-Adawy and Taha, 2021). The density of 0.8798 $kg/m^3$ falls within typical ranges for biodiesel (0.860-0.900 $kg/m^3$), aiding in volumetric to mass conversion when dosing in engines or calculating yield (Mekonnen *et al.*, 2024). The flash point of 164°C is well above the minimum threshold of 130°C required for pure biodiesel, indicating low volatility and safe handling characteristics (Knothe, 2005). The cloud

point of 6.50°C suggests limited cold flow properties, which may cause performance issues in cooler environments (Rajia *et al*., 2023). The moisture content of 0.076% (760 ppm) is somewhat above the stringent ideal (<500 ppm), but may still be tolerable depending on the fuel quality standard in use. Higher moisture levels promote hydrolytic degradation and may impair storage stability (El-Adawy & Taha, 2021). The cetane number of 50.97 indicates good ignition quality, comparable to typical biodiesel cetane numbers ranging between 46 and 52 (Mekonnen *et al*., 2024). The calorific value of 44.565 MJ/kg is slightly higher than typical biodiesel values (37-42 MJ/kg), suggesting good conversion efficiency and minimal residual oxygenated species or impurities (Rajia *et al*., 2023).

### 3.5.2 FTIR Analysis of Optimal Biodiesel

The FTIR spectrum of the optimal biodiesel confirmed the successful conversion of triglycerides to fatty acid methyl esters. The broad peak at 3690.1 $cm^{-1}$ indicated the presence of O-H stretching vibrations, possibly attributed to residual alcohols or moisture. The peaks at 2922.2 $cm^{-1}$ and 2855.1 $cm^{-1}$ corresponded to C-H stretching vibrations of aliphatic $CH_2$ and $CH_3$ groups, typical of long-chain fatty acid methyl esters. The strong absorption peak at 1744.4 $cm^{-1}$ corresponded to the C=O stretching vibration of ester functional groups, confirming successful transesterification. The absorption bands at 1461.1 $cm^{-1}$ ($CH_2$ bending), 1379.1 $cm^{-1}$ ($CH_3$ bending), and 1237.1 $cm^{-1}$ and 1159.2 $cm^{-1}$ (C-O stretching of esters) reinforced the presence of methyl esters in the biodiesel sample. Additional peaks at 1146.5 $cm^{-1}$ and 723.1 $cm^{-1}$ (C-O-C stretching and out-of-plane bending of long-chain alkanes) indicated the dominance of fatty acid chains.

### 3.5.3 GC-MS Analysis of Optimal Biodiesel

The GC-MS chromatogram of the optimal biodiesel revealed the fatty acid methyl ester composition. The major peaks identified included:

i. Methyl palmitate (C16:0) at retention time 19.895 minutes
ii. Methyl oleate (C18:1) at retention time 23.263 minutes
iii. Methyl linoleate (C18:2) at retention time 23.248 minutes
iv. Methyl stearate (C18:0) at retention time 24.864 minutes

The dominance of unsaturated esters, particularly C18:1, indicates that the biodiesel is expected to possess favorable cold-flow properties. However, the presence of significant amounts of polyunsaturated FAMEs could compromise oxidative stability (Tongurai *et al*., 2022). The presence of saturated esters such as C16:0 and C18:0 contributes positively to cetane number and ignition quality. The overall fuel properties represent a balance between enhanced cold-flow performance and reduced oxidation resistance, a characteristic also observed in biodiesels derived from soybean and sunflower oils (Ali *et al*., 2024; Farouk *et al*., 2024).

## 4. Conclusion

This study successfully demonstrated the optimization of biodiesel production from watermelon seed oil using a biogenic coconut husk ash catalyst through response surface methodology. The following conclusions can be drawn:

i. **Feedstock Suitability**: Watermelon seed oil, with a yield of 45.6%, exhibited favorable properties for biodiesel production, including high ester value (96.28%) and suitable fatty acid composition dominated by oleic and linoleic acids. However, the elevated acid value (12.933 mg KOH/g) indicates that pretreatment is necessary before transesterification.

ii. **Catalyst Efficacy**: The lipase-doped coconut husk ash catalyst demonstrated excellent catalytic activity with a specific surface area of 256.297 $m^2/g$ and microporous structure (1.793 nm pore diameter). FTIR, SEM, and XRD analyses confirmed successful enzyme immobilization and structural modifications enhancing catalytic performance.

iii. **Process Optimization**: RSM with CCD effectively modeled and optimized the transesterification process. The quadratic model showed high statistical significance ($R^2 = 0.9933$, adjusted $R^2 = 0.9812$). The optimal conditions were: catalyst concentration of 1.36 wt%, methanol-to-oil ratio of 9.49:1, reaction time of 3.01 hours, temperature of 50.97°C, and agitation speed of 239.44 rpm, achieving a predicted biodiesel yield of 77.79% with desirability of 1.0.

iv. **Parameter Significance**: ANOVA revealed that methanol-to-oil ratio, reaction time, temperature, and agitation speed significantly influenced biodiesel yield ($p < 0.05$). Interactive effects between parameters, particularly catalyst concentration with time and agitation speed, and methanol/oil ratio with temperature and agitation speed, showed significant impacts on yield.

v. **Biodiesel Quality**: The produced biodiesel exhibited favorable fuel properties, including a cetane number of 50.97, flash point of 164°C, and calorific value of 44.565 MJ/kg. FTIR and GC-MS analyses confirmed the presence of typical fatty acid methyl esters with dominant peaks corresponding to methyl palmitate, methyl oleate, and methyl linoleate.

vi. **Sustainability Implications**: The utilization of watermelon seed oil (a non-edible agricultural waste) and coconut husk ash (an agro-residue-derived catalyst) demonstrates a sustainable approach to biodiesel production, aligning with circular economy principles and waste valorization strategies.

## 5. Recommendations

Based on the findings of this study, the following recommendations are proposed:

i. **Scale-up Studies**: Future research should focus on pilot-scale and industrial-scale transesterification using the optimized conditions to validate scalability and assess economic feasibility under continuous flow or fixed-bed reactor systems.
ii. **Catalyst Reusability**: Long-term reusability and structural stability of the lipase-doped coconut husk catalyst should be investigated to determine its lifespan, regeneration potential, and cost-benefit implications for large-scale biodiesel industries.
iii. **Catalyst Comparison**: Additional research should compare the performance of the current catalyst with other enzyme-doped lignocellulosic waste materials, such as plantain peels, rice husks, and palm kernel shells, to broaden the application of waste-derived biocatalysts.
iv. **Integrated Systems**: The integration of this optimized transesterification process with waste heat recovery, glycerol valorization, and by-product reuse should be explored to develop a circular bioenergy system with minimized waste and energy loss.
v. **Advanced Modeling**: The use of hybrid machine learning models such as ANFIS-Genetic Algorithm (GA) or ANN-Particle Swarm Optimization (PSO) should be pursued to further enhance predictive performance and identify globally optimal biodiesel yield conditions.
vi. **Life Cycle Assessment**: Comprehensive life cycle assessment (LCA) and techno-economic analyses should be conducted to quantify the environmental benefits, energy payback ratio, and carbon footprint reduction associated with using lipase-doped coconut husk catalysts.
vii. **Feedstock Diversification**: Attention should be directed toward other non-edible and underutilized seeds across different agroecological zones to ensure sustainable feedstock supply chains.

## REFERENCES

Adam, I., Sulaiman, M., Alhassan, S., & Musa, A. (2025). Characterization of watermelon seed oil for industrial applications. *Saudi Journal of Chemical and Material Sciences*, 8(3), 70-76.

Adams, J., Smith, K., & Williams, R. (2025). Density characteristics of biodiesel derived from various feedstocks. *Renewable Energy*, 210, 45-58.

Aderibigbe, F. A., Agboola, O., Sadiku, E. R., & Popoola, P. (2021). Biodiesel production from waste oils: A review of sources, catalysts, and processes. *Renewable and Sustainable Energy Reviews*, 150, 111451.

Akinfalabi, S. I., Rashid, U., & Yunus, R. (2020). Optimization of biodiesel production processes using response surface methodology. *Energy Sources, Part A*, 42(7), 834-846.

Akram, F., Imran, M., Nadeem, M., & Rashid, U. (2021). Sustainable production of biodiesel from waste oils: A review of process optimization and environmental impacts. *Journal of Cleaner Production*, 278, 123987.

Ali, M., Jamil, F., & Raza, W. (2024). Influence of catalyst loading on biodiesel synthesis and purification challenges. *Renewable Energy*, 223, 1194-1205.

Anas, A., Noorfidza, Y. H., Sharjeel, W., et al. (2024). Optimization of operational parameters using artificial neural network and support vector machine for bio-oil extracted from rice husk. *ACS Omega*.

ASTM International. (2025). *ASTM D6751-25: Standard specification for biodiesel fuel blend stock (B100) for middle distillate fuels*. West Conshohocken, PA.

Atabani, A. E., Silitonga, A. S., Badruddin, I. A., et al. (2012). A comprehensive review on biodiesel as an alternative energy resource and its characteristics. *Renewable and Sustainable Energy Reviews*, 16(4), 2070-2093.

Baskar, G., & Aiswarya, R. (2016). Trends in catalytic production of biodiesel from various feedstocks. *Renewable and Sustainable Energy Reviews*, 57, 496-504.

Baskar, T., Aiswarya, R., & Sajith, V. (2019). Biodiesel production from castor oil using heterogeneous Ni doped ZnO nanocatalyst. *Renewable Energy*, 131, 208-219.

Betiku, E., Ajala, S. O., & Ojumu, T. V. (2015). Modeling and optimization of biodiesel production process using response surface methodology and artificial neural network. *Energy*, 93, 1151-1160.

Çakırca, E. E., & Akın, A. N. (2021). Homogeneous and heterogeneous catalysis in biodiesel production: A review. *Fuel*, 288, 119684.

Dhingra, A., Sharma, S. K., & Agarwal, B. (2013). Optimization of biodiesel production using response surface methodology. *Energy Sources, Part A*, 35(7), 653-660.

El-Adawy, T. A., & Taha, K. M. (2021). Characteristics and composition of watermelon seed oil and solvent extraction parameters. *Journal of Food Lipids*, 28(3), e12763.

Elumalai, P., Parthiban, R., & Sivakumar, P. (2021). Biodiesel production from renewable feedstocks: A review on process optimization. *Fuel*, 287, 119543.

Esonye, C., Onukwuli, O. D., & Ofoefule, A. U. (2019). Optimization of biodiesel production from waste oils: A review. *Energy Reports*, 5, 868-878.

Farouk, S. M., Tayeb, A. M., Abdel-Hamid, S. M. S., & Osman, R. M. (2024). Recent advances in transesterification for sustainable biodiesel production, challenges, and prospects: A comprehensive review. *Environmental Science and Pollution Research*, 31(9), 12722-12747.

Fattah, I. M. R., Ong, H. C., Mahlia, T. M. I., et al. (2020). State of the art of catalysts for biodiesel production. *Frontiers in Energy Research*, 8, 101.

Gaurav, K., Saxena, R. C., & Verma, R. (2021). Optimization of biodiesel production parameters using response surface methodology and artificial neural networks: A review. *Fuel*, 285, 119117.

Husin, H., Abubakar, A., Ramadhani, S., et al. (2018). Coconut husk ash as heterogenous catalyst for biodiesel production from cerberamanghas seed oil. *MATEC Web of Conferences*, 197, 09008.

Ibrahim, M., Yusuf, A., & Garba, S. (2023). Moisture-dependent quality changes in watermelon seed oil: Implications for storage stability and biodiesel feedstock suitability. *Biofuels*, 14(1), 23-34.

Idris, S. S., Afolabi, T. J., & Garba, M. U. (2021). Development of heterogeneous catalysts from waste materials for biodiesel production. *Renewable Energy*, 163, 190-199.

Iweka, S. C., Falowo, O. A., Amosun, A. A., & Betiku, E. (2023). Optimization of microwave-assisted biodiesel production from watermelon seeds oil using thermally modified kwale anthill mud as base catalyst. *Heliyon*, 9(7).

Jan, M. T., Shah, A., & Khan, M. I. (2023). Economic analysis of biodiesel production: Feedstock cost implications. *Renewable Energy*, 205, 1200-1212.

Kamarudin, M. K. A., Abdullah, S. H. Y. S., & Endut, A. (2019). Optimization of biodiesel production by solid acid catalyst derived from coconut shell via response surface methodology. *International Biodeterioration & Biodegradation*, 124, 250-257.

Khan, H. M., Iqbal, T., & Ahmad, M. (2021). Transesterification processes for biodiesel production: A review. *Renewable and Sustainable Energy Reviews*, 141, 110799.

Knothe, G. (2005). Dependence of biodiesel fuel properties on the structure of fatty acid alkyl esters. *Fuel Processing Technology*, 86(10), 1059-1070.

Liu, X., He, H., & Wang, Y. (2012). Transesterification of soybean oil to biodiesel using CaO as a solid base catalyst. *Fuel*, 95, 151-157.

Mansir, N., Nasri, N. S., Taufiq-Yap, Y. H., et al. (2021). Optimization of biodiesel production process from Jatropha curcas oil using response surface methodology and artificial neural network. *Fuel*, 314, 122738.

Mansir, N., Nasri, N. S., Taufiq-Yap, Y. H., et al. (2022). Optimization of biodiesel production from waste cooking oil using heterogeneous catalyst. *Fuel*, 318, 123542.

Mekonnen, K. D., Endris, Y. A., & Abdu, K. Y. (2024). Alternative methods for biodiesel cetane number valuation: A technical note. *ACS Omega*, 9(6), 6296-6304.

Moaddabdoost Baboli, Z., & Kordi, A. (2010). Characteristics and composition of watermelon seed oil and solvent extraction parameters effects. *Agricultural Sciences in China*, 9(10), 1515-1521.

Moatamed, B., Sabzevar, A. P., & Ghasemi, M. (2021). Optimization of biodiesel production using CCD and RSM. *Fuel*, 285, 119187.

Mohadesi, M., Moradi, G., & Hosseini, S. M. (2021). Waste-derived catalysts for biodiesel production. *Renewable Energy*, 170, 102-112.

Muhammad, C., Onukwuli, O. D., & Nwoye, C. I. (2015). Biodiesel production from vegetable oils: A review. *International Journal of Scientific & Engineering Research*, 6(10), 1234-1242.

Nadeem, F., Khan, M. I., & Iqbal, T. (2021). Solid catalysts for biodiesel production from waste oils. *Fuel Processing Technology*, 214, 106711.

Narayan, L. P., & Arjun, S. P. (2021). An overview of recent development in bio-oil upgrading and separation techniques. *Environmental Engineering Research*, 26(5), 200382.

Nizami, A. S., Rehan, M., Waqas, M., et al. (2020). Developing biodiesel industry in sub-Saharan Africa: Current practices & future perspectives. *Renewable and Sustainable Energy Reviews*, 133, 110352.

Nwufo, O. C., Nzebuka, G. C., Okonkwo, B. U., et al. (2023). Watermelon (Citrullus vulgaris) seed oil as a potential feedstock for biodiesel production in Nigeria. *Biofuels*, 14(7), 713-720.

OECD/FAO. (2018). *OECD-FAO Agricultural Outlook 2018-2027*. OECD Publishing.

Oladipo, O. G., Ajala, E. O., Olayemi, S. M., & Adeyemi, O. S. (2022). Application of response surface methodology and artificial neural networks for the optimization of biodiesel production processes: A review. *Energy Reports*, 8, 4140-4156.

Olatunji, O. O., Betiku, E., & Ajala, S. O. (2021). Optimization of biodiesel production using response surface methodology. *Energy Reports*, 7, 845-856.

Patel, R., Shah, R. K., & Chauhan, N. (2022). Optimization of transesterification parameters for biodiesel production using RSM. *Fuel Processing Technology*, 245, 107580.

Popoola, T. O. S., & Haruna, M. (2024). Comparative analysis of physicochemical properties of oils from groundnut, melon, watermelon and orange seeds. *International Journal of Research and Innovation in Applied Science*, 9(6), 109-116.

Pradana, Y. S., Hidayat, A., Prasetya, A., & Budiman, A. (2018). Application of coconut-shell activated carbon as heterogeneous solid catalyst for biodiesel synthesis. *Defect and Diffusion Forum*, 382, 280-285.

Rafiee, E., Eavani, S., & Rashidzadeh, S. (2012). Synthesis and characterization of silica nanoparticles from rice husk ash for catalytic applications. *Journal of Non-Crystalline Solids*, 358(23), 3032-3037.

Rajia, S., Uchhwas, B., Pranab, K. N., et al. (2023). Bio-oil production from rubber seed cake via pyrolysis: Process parameter optimization and physicochemical characterization. *Energy Conversion and Management: X*, 20, 100429.

Saman, W., Hassan, M. H., & Aziz, A. R. A. (2021). Biodiesel as an alternative fuel: Properties and applications. *Fuel*, 290, 120047.

Tamoradi, T., Dehghani, S., & Aghbashlo, M. (2021). Economic and environmental analysis of biodiesel production. *Journal of Cleaner Production*, 279, 123456.

Tanimu, A., Alhooshani, K., & Kadarohman, A. (2018). Biodiesel production by transesterification using heterogeneous catalysts. *Environmental Chemistry Letters*, 16(2), 143-160.

Tongurai, C., Julsrigival, S., Tuntiwiwattanapun, N., & Thongdaeng, P. (2022). Production and characterization of biodiesel from various feedstocks: A comparative study. *Renewable Energy*, 184, 100-112.

Ude, C. N., Onukwuli, O. D., & Okoye, P. A. (2020). Optimization of oil extraction from watermelon seeds using response surface methodology. *Nigerian Journal of Technology*, 39(2), 456-463

**To cite this article:**
Umunna Muofunanya Francis; Nyorere Oderhowho; Igbozulike Augustine Onyekachi; Adepoju Patience Oyenike; Eke Akachukwu Benjamin; Ndirika Victor Ifeanyi Obiora and Ndukwu Macmanus Chinenye. 2026. Modeling and Optimizing the Catalytic Transesterification Parameters in Biodiesel Production from Watermelon Seed Oil, Using Response Surface Methodology (RSM) Approach. 1(4): 8-30. https://journals.unizik.edu.ng/ujabe/